

A Composite Reaction Engineering Approach to Drying of Aqueous Droplets Containing Sucrose, Maltodextrin (DE6) and Their Mixtures

Kamlesh C. Patel, Xiao Dong Chen, and Sean X. Q. Lin

Biotechnology and Food Engineering Group, Dept. of Chemical Engineering, Monash University, Melbourne, Victoria 3800, Australia

Benu Adhikari

School of Science and Engineering, University of Ballarat, Ballarat, Victoria 3353, Australia

DOI 10.1002/aic.11642

Published online December 5, 2008 in Wiley InterScience (www.interscience.wiley.com).

Recently, several studies have been published on the spray drying of sucrose and other low-molecular-weight sugars which are typically sticky materials. Sticky materials can not be processed under normal drying conditions and may require addition of high-molecular-weight carbohydrates such as maltodextrin. Predicting appropriate drying conditions are however difficult due to the unavailability of drying kinetics. In this article, we have formulated the drying kinetics model using the reaction engineering approach (REA) for the drying of aqueous sucrose and aqueous maltodextrin (DE6) droplets. The relative activation energy was empirically obtained based on experimental measurements. To model the drying of droplets containing both solutes (sucrose and maltodextrin), a new "composite" REA has been established and presented here for the first time. Results demonstrated that the composite REA forms a reliable framework to model the drying of aqueous solutions of pure carbohydrates and their mixtures. © 2008 American Institute of Chemical Engineers AIChE J, 55: 217–231, 2009

Keywords: droplet drying, drying kinetics, sucrose, maltodextrin, sugar mixtures, reaction engineering approach

Introduction

Sucrose and their derivatives are widely used as sweeteners in various food, beverages, bakery, and confectionary products. Amorphous sucrose is commonly used in food and pharmaceutical industries to enhance the dissolution of bulk powders and to carry flavor, drug, and vitamins molecules.^{1,2} The amorphous form has also been reported as essential for

maximizing the stability of proteins, vitamins, and other bioactive molecules in dried products.³ When bioactive molecules are trapped within the rigid amorphous structure, natural degradation processes can greatly be retarded. If crystallization occurs during processing, the water rejected during crystallization may trigger physical changes, chemical reactions, and biochemical degradation leading to a degraded sticky product. Unwanted crystallization is frequently encountered during freeze drying of sugar-rich products which contain low-molecular-weight carbohydrates such as fructose, mannitol and sucrose.

Spray drying is a fast and economical process to manufacture amorphous sucrose because this technique allows for

Correspondence concerning this article should be addressed to X. D. Chen at dong.chen@eng.monash.edu.au.

the rapid removal of water from droplets during processing. Sucrose is considered to be a sticky material and hence the drying of sucrose is not straightforward.⁴ An attempt to dry sucrose in a pure form will lead to the formation of a sticky material or large lumps/cake.^{5,6} The sticky behavior of products can result in heavy deposition of the product on dryer walls, lower yields, difficulty in handling the product and can also pose fire hazards. These problems are normally overcome to a certain extent by mixing drying aids with sucrose solutions before drying. Partially hydrolyzed starch derivatives such as maltodextrin are commonly used as drying aids during spray drying of sugar-rich materials such as fructose, glucose, sucrose, honey, and acid-rich foods such as fruit and vegetable juices.^{7,8}

Prevention of stickiness during drying of sugar-rich materials such as sucrose requires knowledge of the drying characteristics of materials with respect to the dryer's humidity and temperature, as well as knowledge of the conditions that govern the stability of the product. To understand the sticky behavior of amorphous carbohydrates and other low-molecular-weight sugars during spray drying, the glass transition temperature (T_g) has frequently been used in the literature.^{4,9–15} When the product temperature of the amorphous glassy structure reaches the corresponding T_g , a glassy state transforms into a rubbery state with a sudden reduction in the material viscosity. This leads to a rapid increase in the moisture mobility within the solid matrix, promoting drastic changes to physical and chemical properties of the material.^{11,15} To obtain a stable nonsticky product, the product temperature must be lower than the corresponding T_g by 10–20°C.^{4,9,13} It is therefore essential to evaluate transient changes in T_g during spray drying. Prediction of T_g following the complete drying process requires the drying kinetics model because T_g is mainly affected by the droplet's moisture content.

The main aim of this study is to formulate a simple and effective drying kinetics model for the convective air drying of aqueous sucrose solutions and maltodextrin solutions. An accurate drying kinetics model can deliver optimum drying conditions which may favor higher-stability products and minimum wall depositions in the dryer. In the literature, few studies have reported the formulation of comprehensive drying kinetics models for the drying of aqueous sucrose or sucrose/maltodextrin mixtures. Adhikari et al.^{4,9} evaluated drying kinetics of sugar droplets using a diffusion model. Predictions by this diffusion model requires solving partial differential equations and careful estimation of moisture diffusivity that should be a function of the droplet's temperature and moisture content. The diffusion model was validated using data measured from laboratory experiments on the hot air drying of single suspended droplets. The average and maximum relative errors when matching measured droplet moisture content data and predicted data were reported to be 4.5–6% and 9–11%, respectively.^{4,9} It was observed in their work, that the predicted moisture content profiles using the diffusion-based drying kinetics model overestimated measured moisture content profiles under laboratory conditions tested by Adhikari et al.^{4,9}

In this study, we aim to formulate the drying kinetics model for the convective drying of sucrose, maltodextrin, and their mixtures using the reaction engineering approach (REA). The REA is a simple and effective approach to

model the drying process for aqueous materials. This kind of model is normally desirable for fast and effective modeling of drying processes by various process computation tools. The REA was first reported around 10 years ago by Chen and Xie¹⁶ to model the air drying of small droplets and thin-layer materials. Over the last decade the REA has successfully been used to develop drying kinetics of common dairy materials such as skim milk, whole milk, cream, lactose and whey proteins concentrate.^{17–19} To model the drying of droplets containing two solutes, i.e. sucrose-maltodextrin mixtures of different weight proportions, a new “composite” REA is developed in this article. Unlike the previous REA, the effect of the initial moisture content on the drying rate is taken into account. Experimental data reported by Adhikari et al.^{4,9} were used in this study to formulate the REA-based drying kinetics model. The fundamental basis and the governing equations of the REA are briefly described in the “Mathematical model” section.

Mathematical Model

Reaction engineering approach

The reaction engineering approach (REA) is a semiempirical model that holds a physical meaning of the droplet drying process. The REA predicts average characteristics of the material during drying and hence may be classified as the “lumped-parameter” model. The REA was formulated based on the reaction engineering concept, which considered evaporation as an activation process that must overcome the energy barrier for water removal during drying, whilst wetting is not an activation process and therefore does not encounter such an energy barrier.¹⁶

Chen and Xie¹⁶ originally proposed the REA to model the convective air drying of kiwifruit skin, apple, and potato slices and silica gel particles. Chen and Lin¹⁷ modified this approach to form a more accurate model by measuring key drying/droplet parameters directly from single droplet drying experiments. Chen and Lin¹⁷ compared predictions delivered by the REA and the characteristic drying rate curve (CDRC) model for the drying of skim milk and whole milk droplets, and found the REA to be more accurate compared to the CDRC model for all sets of drying conditions tested in the laboratory. The fundamentals of the CDRC model and the REA are comprehensively elaborated and compared by Chen.²⁰ Recently the REA was successfully employed to predict the drying behavior of lactose, cream and whey proteins concentrate with high accuracy.^{18,19} Patel and Chen^{21–23} employed the REA-based drying kinetics model to conduct detailed spray drying modeling and dryer-wide simulations using industrial spray drying conditions for the drying of skim milk, lactose, and whey proteins concentrate. In their studies the sensitivity of the REA to important drying parameters and droplet characteristics was examined. The REA was found to be sensitive to all process and feed parameters, and useful to understand the variations in product properties upon changing operating conditions and feed parameters.

To formulate a mathematical expression the REA used a vapor concentration difference to characterize the driving force for the removal of moisture from the droplet surface. Under drying conditions the drying rate can be expressed by the following formulae:

$$-\frac{dm_p}{dt} = h_m A_p (\rho_{v,s} - \rho_{v,b}) \quad (1)$$

where $\rho_{v,s}$ (kg m^{-3}) is the vapor concentration at the droplet surface, $\rho_{v,b}$ (kg m^{-3}) is the vapor concentration of bulk drying gas, h_m (m s^{-1}) is the mass-transfer coefficient, A_p (m^2) is the droplet's surface area and m_p (kg) is the droplet weight. The rate of change of droplet weight during drying requires these time-dependent parameters to be known during drying. The negative sign on the left hand side of Eq. 1 indicates the reduction of the droplet's weight during drying. The parameter $\rho_{v,s}$ is difficult to measure from experiments due to the rapid change in the moisture content at the droplet surface. However, it is known that $\rho_{v,s}$ should be equal to the saturated vapor concentration ($\rho_{v,\text{sat}}$) when the droplet surface is fully saturated with free water (i.e. during constant drying rate period), and should be smaller than $\rho_{v,\text{sat}}$ during the falling drying rate period. The parameters $\rho_{v,s}$ and $\rho_{v,\text{sat}}$ can be correlated, and the relationship between $\rho_{v,s}$ and $\rho_{v,\text{sat}}$ was expressed using the following expression^{16–19}:

$$\rho_{v,s} = \text{RH}_s \rho_{v,\text{sat}}(T_s) \quad (2)$$

where RH_s (in fraction) is the relative humidity or water activity at the droplet surface and T_s is the surface temperature. The droplet surface temperature T_s may be considered as the average droplet temperature (T_p) if temperature nonuniformity within the droplet is negligible. The surface relative humidity (RH_s) is clearly a function of surface water content and surface temperature and was expressed using the following expression^{16,17}:

$$\text{RH}_s = \exp \left(-\frac{\Delta E_v}{R_g T_p} \right) \quad (3)$$

where ΔE_v (J mol^{-1}) is the parameter which can be correlated with the average moisture content of the droplet/particle. The parameter ΔE_v was quoted as the apparent activation energy that represents the extent of difficulty when removing moisture from the droplet during drying. From Eq. 3, the apparent activation energy for drying (ΔE_v) can be expressed as:

$$\Delta E_v = -R_g T_p \ln(\text{RH}_s) \quad (4)$$

Thus, the apparent activation energy reflects the vapor concentration depression ($\text{RH}_s = \rho_{v,s}/\rho_{v,\text{sat}}$) at the droplet surface during drying. Using Eqs. 1–3, the relation between the drying rate and the apparent activation energy can be expressed as:

$$\begin{aligned} -\frac{dm_p}{dt} &= -\frac{dm_w}{dt} = -m_{\text{solids}} \frac{d\bar{X}}{dt} \\ &= h_m A_p \left[\rho_{v,\text{sat}} \exp \left(-\frac{\Delta E_v}{R_g T_p} \right) - \rho_{v,b} \right] \end{aligned} \quad (5)$$

where m_w (kg) is the mass of water in the droplet and \bar{X} ($\text{kg water kg dry solids}^{-1}$) is the droplet's average moisture content. The first term on the right hand side of Eq. 5 ($\rho_{v,\text{sat}}$

terms) is the zero order drying “reaction” that is the activation process.¹⁶ The second term on the right ($\rho_{v,b}$ terms) is the first order wetting “reaction.”¹⁶ Thus, the rate of moisture removal was seen as a competitive process between drying and wetting reactions. The drying rate of the liquid droplet can be estimated using Eq. 5 if ΔE_v is known as a function of the droplet's moisture content. If ΔE_v for the specific material is unknown, it can be determined by obtaining required parameters dm_p/dt , h_m , A_p , T_p , and $\rho_{v,b}$ from the droplet drying experiment. Eq. 5 may be re-written to estimate ΔE_v from experimental measurements:

$$\Delta E_v = -R_g T_p \ln \left(\frac{\rho_{v,b} - \frac{dm_p/dt}{h_m A_p}}{\rho_{v,\text{sat}}} \right) \quad (6)$$

The vapor density of the drying medium ($\rho_{v,b}$) may be estimated using the ideal gas law and gas temperature conditions. The saturated vapor density at the droplet surface ($\rho_{v,\text{sat}}$) can be estimated using the droplet surface temperature (T_s). The relationship between $\rho_{v,\text{sat}}$ and T_s (K) may be expressed using the following correlation²⁴:

$$\begin{aligned} \rho_{v,\text{sat}} &= 4.8444 \times 10^{-9} (T_s - 273.15)^4 \\ &\quad - 1.4807 \times 10^{-7} (T_s - 273.15)^3 \\ &\quad + 2.6572 \times 10^{-5} (T_s - 273.15)^2 \\ &\quad - 4.8613 \times 10^{-5} (T_s - 273.15) + 8.3420 \times 10^{-3} \end{aligned} \quad (7)$$

Equation 7 was formulated by correlating $\rho_{v,\text{sat}}$ and temperature data (for $273.15 \text{ K} < T < 430 \text{ K}$) reported by Incropera and DeWitt.²⁵ In Eq. 7 T_s may be replaced with T_p if temperature distribution within the droplet is negligible. The mass-transfer coefficient (h_m) of the spherical droplet may be approximated using the following correlation²⁶:

$$\text{Sh} = \frac{h_m d_p}{D_v} = 1.63 + 0.54 (Re)^{1/2} (Sc)^{1/3} \quad (8)$$

where D_v ($\text{m}^2 \text{ s}^{-1}$) is the air-vapor diffusion coefficient. For materials which do not have the apparent activation energy measured previously, it can be estimated using Eq. 6 and measured droplet weight, temperature, and diameter profiles from the droplet drying experiments.

In the literature the apparent activation energy (ΔE_v) was normalized using the “equilibrium” or “maximum” activation energy ($\Delta E_{v,b}$), thus yielding the “relative activation energy” ($\Delta E_v/\Delta E_{v,b}$). The apparent activation energy (ΔE_v) becomes the “maximum” or “equilibrium” activation energy ($\Delta E_{v,b}$) when the relative humidity at the droplet surface is in equilibrium with the bulk drying gas relative humidity. At this equilibrium point the drying rate will be zero. The relative activation energy ($\Delta E_v/\Delta E_{v,b}$) can be correlated with the droplet's average moisture content ($\bar{X} - X_b$), as previously done in the literature^{17–19}:

$$\frac{\Delta E_v}{\Delta E_{v,b}} = f(\bar{X} - X_b) \quad (9)$$

where X_b is the equilibrium moisture content (kg kg^{-1} , dry basis) that can be obtained from the moisture isotherm model

of corresponding materials.^{16,17} When the droplet surface is saturated with free water (i.e. \bar{X} is high), the relative activation energy ($\Delta E_v/\Delta E_{v,b}$) and hence the difficulty in removing the free moisture is expected to be very small. The relative activation energy gradually increases to a larger value when the droplet's moisture content is reduced during drying. At the zero free moisture content (i.e. $\bar{X} = X_b$), $\Delta E_v/\Delta E_{v,b}$ is expected to be unity. Here, the relationship between the relative activation energy ($\Delta E_v/\Delta E_{v,b}$) and the droplet's moisture content ($\bar{X} - X_b$) under drying conditions can be viewed as a characteristic property or a "fingerprint" of the individual material. This characteristic property must be obtained from the experimental work for any specific material of concern. Once the relationship between the relative activation energy and the material's moisture content defined by Eq. 9 is established, the drying rate or the average moisture content of moist materials can be predicted at any location in the spray dryer using Eq. 5. This REA-based drying kinetics model, developed from laboratory experiments, may be used for simulating industrial spray drying of the same material for product characterization, process optimization, scale-up, and designing purposes.

The parameter $\Delta E_{v,b}$ in Eq. 9 was correlated with the gas relative humidity (RH_b) and the gas temperature (T_b), and was expressed using the similar expression presented by Eq. 4:

$$\Delta E_{v,b} = -R_g T_b \ln(RH_b) \quad (10)$$

where

$$RH_b = \frac{\rho_{v,b}(T_b)}{\rho_{v,sat}(T_b)} \quad (11)$$

Chen and Lin¹⁷ performed experiments on the drying of skim milk and whole milk droplets using hot air of constant air temperature (variation $\pm 0.4^\circ\text{C}$) and humidity (negligible variation) to evaluate the relative activation energy-moisture content relationship. As an example, the "fingerprint" of skim milk was described using the following correlation¹⁷:

$$\frac{\Delta E_v}{\Delta E_{v,b}} = C_1 \exp[-C_2(\bar{X} - X_b)^{C_3}] \quad (12)$$

where C_1 , C_2 , and C_3 are model coefficients, which were reported to be 0.998, 1.405, and 0.93, respectively for the drying of skim milk droplets. The relative activation energy was estimated using Eqs. 6 and 10 and experimental data collected from the isothermal drying of skim milk droplets of 20 wt % ($\bar{X}_0 = 4.0 \text{ kg} \cdot \text{kg}^{-1}$) and 30 wt % ($\bar{X}_0 = 2.33 \text{ kg} \cdot \text{kg}^{-1}$) initial solids contents. The single correlation was employed by Chen and Lin¹⁷ to evaluate the fingerprint for skim milk droplets of two different initial moisture contents as shown in Figure 1. This approach is reasonable to model the material with high initial moisture concentrations. However, when drying the droplets of low initial moisture contents, as an example $\bar{X}_0 = 1.0 \text{ kg} \cdot \text{kg}^{-1}$, the single fitting curve shown in Figure 1 may introduce some errors during the earlier drying stage because the model would predict a high relative activation energy at the beginning of drying. The relative activation energy should be close to zero due to the presence of some free moisture on the droplet surface at the beginning of drying. Therefore, the

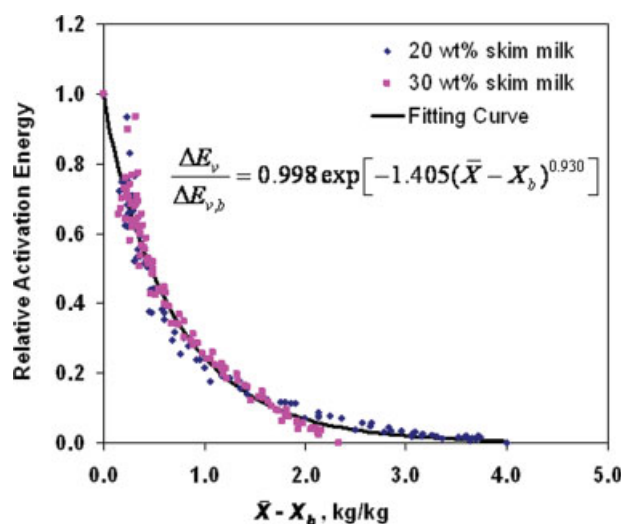


Figure 1. The relative activation energy ($\Delta E_v/\Delta E_{v,b}$) against the droplet's moisture content for the drying of aqueous skim milk droplets of different initial moisture contents.¹⁷

[Color figure can be viewed in the online issue, which is available at www.interscience.wiley.com.]

single correlation approach is likely to overestimate the relative activation energy, and hence underestimate the average drying rate during the earlier drying stage for the drying of droplets of low initial moisture contents. Experimental results (see Figure 1) of Chen and Lin¹⁷ suggest that the relative activation energy should be a function of the droplet's initial moisture concentration. In this study, an attempt is made for the first time to account for the effect of the initial moisture content explicitly on the REA-based drying kinetics model.

Heat transfer model

The time-dependent temperature profile of spherical droplets was approximated by evaluating heat balance over the single droplet considering the droplet is a binary system made of solids and water:

$$\frac{dT_p}{dt} = \frac{hA_p(T_b - T_p) + \Delta H_v \frac{dm_w}{dt}}{(m_{\text{solids}}C_{p,\text{solids}} + m_w C_{p,w})} \quad (13)$$

The use of Eq. 13 requires the assumption of uniform temperature within the droplet to be justified. In this work, experimental data on the drying of sucrose-maltodextrin droplets were obtained from Adhikari et al.^{4,9} They assumed uniform temperature within droplets of the initial diameter in the range of 2.2–2.4 mm when formulating the drying kinetics model in their studies. For the same droplets and drying conditions used in this study, Adhikari et al.^{4,9} reported the average heat-transfer Biot number during the entire drying period varied from 0.07 to 0.11. The modified Biot number analysis,^{27,28} which is more logical for the droplet drying process and accounted for the evaporative effect, would yield Biot numbers even lower than those predicted by Adhikari et al.,^{4,9} thus giving more "freedom" to use the assumption of uniform temperature within the material.²⁹ The heat-transfer Biot number was close to the critical value

Table 1. Thermophysical Properties Used in Calculations

Heat capacity (J kg ⁻¹ K ⁻¹)	
Air*	$1.9327 \times 10^{-10}T^4 - 7.9999 \times 10^{-7}T^3 + 1.1407 \times 10^{-3}T^2 - 0.4489T + 1057.3$ (295 K < T < 800 K, $R^2 = 0.9995$)
Water (liquid)*	$1.9211 \times 10^{-6}T^4 - 2.5648 \times 10^{-3}T^3 + 1.2905T^2 - 289.55T + 28586$ (295 K < T < 370 K, $R^2 = 0.9992$)
Sucrose [†]	$4.4369T + 1121.3$
Maltodextrin (DE6) [†]	$3.5242T + 1319.7$
Air* Viscosity (MPa s ⁻¹)	$-0.000037T^2 + 0.0687T + 0.885$ (250 K < T < 400 K, $R^2 = 0.9996$)
Thermal conductivity (W m ⁻¹ K ⁻¹)	
Air*	$0.0000778T + 0.00274$ (250 K < T < 400 K, $R^2 = 0.9996$)
Water (liquid)*	$0.57109 + 0.0017625T - 6.7036 \times 10^{-6}T^2$
Sucrose [†]	0.277
Maltodextrin (DE6) [†]	0.187
Density (kg m ⁻³)	
Air*, [§]	$(273.15 \times \rho_{\text{air}} \text{ at } 273.15 \text{ K})/T$
Water (liquid)*	$997.18 + 0.0031439T - 0.0037574T^2$
Sucrose [†]	1587
Maltodextrin (DE6) [†]	1410
Vapor-air diffusivity* (m ² s ⁻¹)	$1.963 \times 10^{-7}T - 3.33307 \times 10^{-5}$ (293 K < T < 373 K, $R^2 = 1.0$)
Latent heat of vaporization* (J kg ⁻¹)	$3,158,100 - 2401.8T$ (290 K < T < 370 K, $R^2 = 0.9997$)

*Correlations were obtained by plotting the temperature and the property reported by Incropera and DeWitt.³⁰

[†] T is in °C, obtained from Adhikari et al.⁴

[‡] T is in °C, obtained from Choi and Okos.²⁵

[§]At $T = 273.15$ K, $\rho_{\text{air}} = 1.2928$ kg m⁻³.

of 0.1 during the drying process, hence it is reasonable to adopt the heat-transfer model described by Eq. 13.

During the droplet drying experiment in the laboratory, the droplet is normally suspended on a thin glass filament. It is expected that a fraction of the heat may be conducted through the filament during drying. Adhikari et al.^{4,9} accounted for the heat conducted through the filament when formulating the heat-transfer model in their studies. It was found during simulations in this study that the average difference between predicted droplet temperatures with and without considering the heat conduction through the filament was only 0.5°C. Therefore, the heat conduction through the glass filament was assumed to be negligible during all simulation runs in this study.

The heat-transfer coefficient h (W m⁻² K⁻¹) in Eq. 13 was estimated using the following modified Ranz-Marshall correlation²⁶:

$$Nu = \frac{h \cdot d_p}{k_b} = 2.04 + 0.62(Re)^{1/2}(Pr)^{1/3} \quad (14)$$

The required drying gas properties (viscosity, thermal conductivity, density, and water-air diffusivity) for estimating h , h_m and other thermophysical properties were calculated using appropriate correlations presented in Table 1.

Moisture desorption isotherms

The equilibrium moisture content for the drying of pure sucrose droplets was estimated using the following Norrish model, which is a semiempirical modification of Raoult law^{4,31,32}:

$$a_w = \psi_w \exp(-K_N(1 - \psi_w)^2) \quad (15)$$

where ψ_w is the molar fraction of water in a single droplet, a_w is the water activity of the droplet and K_N is the Norrish equation coefficient. The equilibrium moisture content can be

calculated from ψ_w . For pure sucrose, the coefficient K_N was reported to be 2.6 by Norrish,³¹ 2.7 by Toledo³² and 6.22 by Adhikari.³³ In this work, the K_N value reported by Adhikari³³ was chosen. To obtain the equilibrium moisture content for the drying of aqueous maltodextrin (DE6) droplets, the following Guggenheim-Anderson-deBoer (GAB) model was used^{4,33}:

$$X_b = \frac{m_0CKa_w}{(1 - Ka_w)(1 - Ka_w + CKa_w)} \quad (16)$$

where X_b is the equilibrium moisture content, and m_0 , C , and K are equation coefficients. These equation coefficients were measured through independent experiments by Adhikari et al.,⁴ and reported as $m_0 = 0.04$, $C = 30$, and $K = 0.98$ for pure maltodextrin (DE6) droplets. The range of air temperature and relative humidity for validating the aforementioned model is however not reported by Adhikari et al.⁴ GAB parameters C and K are normally expressed as a function of the material's temperature, but such expressions are not available in literature for aqueous maltodextrin (DE6). The equilibrium moisture content (X_b) of the aqueous droplet containing two different solutes, for instance sucrose and maltodextrin, were calculated using the equilibrium moisture content and the mass fraction of each solute as:

$$X_{b,\text{mixture}} = \omega_{\text{sucrose}}X_{b,\text{sucrose}} + \omega_{\text{maltodextrin}}X_{b,\text{maltodextrin}} \quad (17)$$

The estimated equilibrium moisture content of aqueous droplets containing sucrose, maltodextrin, and their mixtures under the drying conditions used in this study is reported in Table 2.

Shrinkage model

Formulating the drying kinetics model requires the droplet's shrinkage behavior during drying. Empirical or semiempirical shrinkage models are not available in the literature for the drying of aqueous droplets containing sucrose, maltodextrin, and their mixtures. The change in droplet diameter

during the drying of single sucrose-maltodextrin droplets were not reported by Adhikari et al.^{4,9} Adhikari et al.⁹ however presented the images of aqueous droplets of three different sucrose-maltodextrin compositions at the beginning and end of drying processes (refer to Figure 2 from Adhikari et al.⁹). Based on these images, the droplet diameter was estimated using the ImageJ (1.37 v) software at the start and end of drying. It was assumed that the relative droplet diameter (d/d_0) varies linearly with the relative droplet moisture content (X/X_0) during the drying of aqueous sucrose-maltodextrin droplets. Based on this assumption, the following linear shrinkage model, similar to that evaluated by Chen and Lin¹⁷ and Lin and Chen,^{18,19,34} was worked out for the drying of droplets containing both sucrose and maltodextrin:

$$\frac{d}{d_0} = \beta + (1 - \beta) \frac{X}{X_0} \quad (18)$$

where the parameter β is the empirical coefficient. The parameter β for sucrose-maltodextrin droplets of different initial compositions is illustrated in Table 3. As Adhikari et al.⁹ did not report the images of pure sucrose droplets and pure maltodextrin droplets during drying, the parameter β for aqueous droplets of individual solutes could not be evaluated.

In this study, both the perfect shrinkage model and the linear shrinkage model were employed to estimate the change in droplet diameter for one drying case in order to compare their effects on the prediction. The shrinkage model which provides higher accuracy of prediction will be used for all other simulation runs. The linear shrinkage model, illustrated by Eq. 18, may give the upper bound of the droplet diameter, whilst the perfect shrinkage model is likely to estimate the lower bound of the droplet diameter during drying. The droplet diameter profile and the sensitivity of both shrinkage models were compared and checked for one drying case in the "Discussion" section.

It was assumed that the droplet remained spherical during the entire period of drying. It should be noted that the droplet may lose its spherical shape as drying proceeds during single droplet drying experiments.^{4,9,26,33–35} This deviation from the sphericity may affect the effective area for heat and mass transfers. However, it is difficult to measure the deviation in the droplet's sphericity from experiments for the size of the droplets used in the laboratory or in the industry. The spherical particle assumption is normally considered to be reasonable for modeling the droplet drying process.

Table 2. Equilibrium Moisture Content (X_b) for Aqueous Droplets of Sucrose:Maltodextrin (S:M) Mixtures

S:M Weight Ratio	X_b (kg kg ⁻¹)	
	RH = 2.0% $T_b = 95^\circ\text{C}$	RH = 2.5% $T_b = 63^\circ\text{C}$
1:0	0.0270	0.0294
4:1	0.0215	0.0235
1:1	0.0135	0.0147
1:4	0.0054	0.0058
0:1	0.00001	0.00001

Table 3. Empirical Parameter β to be Used in the Linear Shrinkage Model for the Drying of Aqueous Droplets Containing Sucrose-Maltodextrin Mixtures

S:M Weight Ratio	Parameter β
4:1	0.9132
1:1	0.8141
1:4	0.7820

Experimental Data

Precise measurements of drying parameters from the experiments are crucial to formulate an accurate correlation between $\Delta E_v/\Delta E_{v,b}$ and $\bar{X}-X_b$. Experimental data on the drying of single suspended droplets of sucrose (S), maltodextrin (M), and their mixtures (S-M) are provided by Dr. Benu Adhikari (senior lecturer, Ballarat University, Australia). Drying conditions and initial droplet characteristics for individual materials used in this study are listed in Table 4. These experimental data have been published in various literatures.^{4,9,33} The experimental set-up, the air humidity measurement procedure and the droplet's temperature and weight measurement techniques during the drying of single suspended droplets are described by Adhikari et al.^{4,9} and are not reported here. In this study the drying kinetics model is formulated for the drying of pure sucrose solution (S:M = 1:0), pure maltodextrin solution (S:M = 0:1) and three different compositions of sucrose-maltodextrin mixtures (S:M = 4:1, S:M = 1:1, S:M = 1:4; all weight ratios). Changes in the droplet's temperature and weight were recorded for aqueous droplets of 1.5 kg kg⁻¹ and 1.0 kg kg⁻¹ (dry basis) initial moisture contents. Droplets were dried using hot air of 1.0 m s⁻¹ velocity and two different temperature and relative humidity (RH) conditions: (1) 63 ± 1°C with 2.5 ± 0.5 %RH; and (2) 95 ± 2°C with 2.0 ± 0.5 %RH. Reported deviations during recording air temperatures (±1–2°C) and air RH (±0.5%) may significantly influence the air absolute humidity and hence the model prediction. The sensitivity of the model prediction to these deviations during the measurement of air properties are not reported by Adhikari et al.,^{4,9} but will be checked in this study.

The relative humidity of hot air was measured by Adhikari et al.^{4,9} by conducting independent experiments on the drying of pure water droplets. During these experiments the same initial droplet volume was used as those reported for sucrose-maltodextrin droplets. The hot air temperature and droplet temperature profiles were recorded during the drying of water droplets. The RH of hot air was calculated using the dry-bulb temperature of hot air and the corresponding wet-bulb temperature of the water droplet (i.e. droplet temperature during the constant temperature period of the drying process). This technique is particularly useful when the RH of hot air is less than 5%. Commercial relative humidity sensors with available accuracy may introduce large errors when measuring RH in the range of 1% to a few percentages.

Deriving the Relative Activation Energy Relationship

Equations 6 and 10 can be used to calculate ΔE_v and $\Delta E_{v,b}$, respectively and thus the relative activation energy

Table 4. Drying Conditions Used for the Drying of 40 wt % ($X_0 = 1.5 \text{ kg kg}^{-1}$, Dry Basis) and 50 wt % ($X_0 = 1.5 \text{ kg kg}^{-1}$, Dry Basis) Aqueous Droplets Containing Sucrose (S), Maltodextrin (M) and Their Mixtures

S:M Weight Ratio	Air Temp. (°C)	Air RH (%)	Initial Drop Diameter (mm)		Initial Drop Temperature (°C)	
			$X_0 = 1.5 \text{ kg kg}^{-1}$	$X_0 = 1.0 \text{ kg kg}^{-1}$	$X_0 = 1.5 \text{ kg kg}^{-1}$	$X_0 = 1.0 \text{ kg kg}^{-1}$
1:0	63	2.5	2.179	2.145	24.48	24.09
	95	2.0	2.179	2.145	25.33	28.00
4:1	63	2.5	2.185	2.154	23.33	23.67
	95	2.0	2.185	2.154	25.81	26.31
1:1	63	2.5	2.196	2.167	23.41	23.92
	95	2.0	2.196	2.167	26.14	25.53
1:4	63	2.5	2.206	2.180	23.52	24.63
	95	2.0	2.206	2.180	26.91	25.91
0:1	63	2.5	2.214	2.188	23.56	22.03
	95	2.0	2.214	—	25.22	—

Hot air velocity was 1.0 m s^{-1} for all the drying runs.

($\Delta E_v/\Delta E_{v,b}$). As mentioned previously, the droplet's weight loss (dm_p/dt), temperature (T_p) and diameter (d_p) profiles along with the air temperature (T_b) and relative humidity (RH) must be used as inputs to the model. In this study, all required parameters except the droplet's diameter change profiles were directly measured from laboratory experiments on the convective isothermal drying of single suspended droplets. The droplet diameter profile was obtained using either the linear shrinkage model or the perfect shrinkage model, described in the "Mathematical model" section. Air temperature and relative humidity are assumed to be constant throughout drying. To obtain the relative activation energy-moisture content relationship, $\Delta E_v/\Delta E_{v,b}$ is plotted against the droplet's moisture content ($\bar{X}-X_b$). In the following subsections the relative activation energy relationship is presented for the drying of aqueous sucrose-maltodextrin droplets.

Aqueous sucrose droplets

The relative activation energy-moisture content relationship for aqueous sucrose droplets of 1.5 kg kg^{-1} and 1.0 kg kg^{-1} (dry basis) initial moisture contents which were dried using hot air of two air temperatures 63°C and 95°C is illustrated in Figure 2. The nature of the experimental relative activation energy in Figure 2 illustrates that the idea of using the single fitting curve, as shown in Figure 1, to correlate relative activation energy data for different initial moisture contents may not be a suitable one. To account for the effect of the initial moisture content on the drying rate, the individual curve for the specific initial moisture content should be used. This approach will provide more accurate predictions. The following simple correlation was found to be suitable for correlating $\Delta E_v/\Delta E_{v,b}$ and $\bar{X}-X_b$ for aqueous sucrose droplets:

$$\frac{\Delta E_v}{\Delta E_{v,b}} = \exp(-(\bar{X}-X_b)^{C_1}) - C_2(\bar{X}-X_b)^2 \quad (19)$$

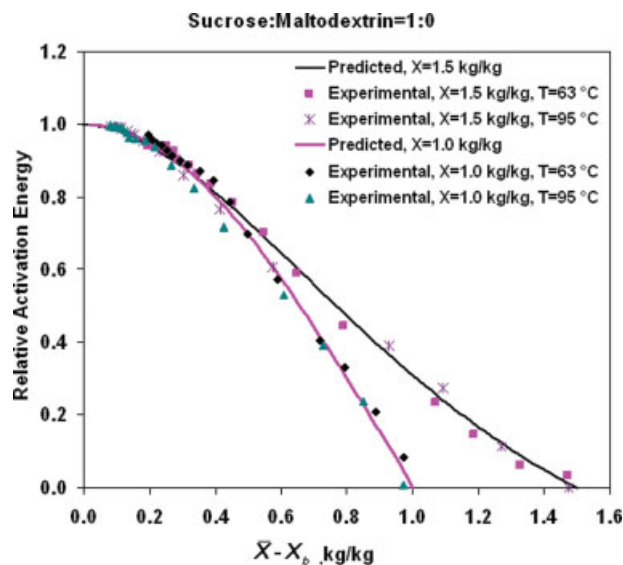


Figure 2. Experimental relative activation energy and fitted curves for the drying of aqueous sucrose droplets (S:M = 1:0) using 63 and 95°C air temperature conditions.

[Color figure can be viewed in the online issue, which is available at www.interscience.wiley.com.]

where C_1 and C_2 are model coefficients and can be obtained from the fitted curve corresponding to the droplet of the specific initial moisture content. Coefficients C_1 and C_2 and R^2 values for aqueous sucrose droplets of 1.0 kg kg^{-1} and 1.5 kg kg^{-1} initial moisture concentrations are listed in Table 5. These coefficients C_1 and C_2 may be expressed as a function of the material's initial moisture content (X_0). Since experimental data are available for the sucrose droplet of only two different X_0 , one can extrapolate only the linear trend.

The relative activation energy curve for the droplet of the highest initial moisture content can be viewed as a so-called "mother" curve. In the present case regarding the drying of sucrose droplets, the relative activation energy curve for the aqueous sucrose droplet of 1.5 kg kg^{-1} initial moisture content can be considered as the "mother" curve. For materials of lower initial moisture contents (e.g. $X_0 = 1.0 \text{ kg kg}^{-1}$), the corresponding relative activation energy curve seemed to be "far away" from the mother curve during the earlier drying stage, but appeared to be getting closer to the mother curve as drying continued, and merged with the mother curve during the later drying stage (see Figure 2). This observation suggests that the degree of difficulty during water evaporation from the droplets of different initial solids contents (or moisture concentrations) is different during the earlier drying

Table 5. Relative Activation Energy Coefficients for Aqueous Sucrose and Maltodextrin (DE6)

	Pure Sucrose		Pure Maltodextrin (DE6)	
	$X_0 = 1.5 \text{ kg kg}^{-1}$	$X_0 = 1.0 \text{ kg kg}^{-1}$	$X_0 = 1.5 \text{ kg kg}^{-1}$	$X_0 = 1.0 \text{ kg kg}^{-1}$
Coefficient C_1	1.777	2.060	0.03447	0.9438
Coefficient C_2	0.05746	0.3593	8.2950	8.8240
Coefficient C_3	—	—	0.5353	0.6030
Coefficient C_4	—	—	1.6860	2.0240
R^2	0.9986	0.9961	0.9972	0.9966
RMSE	0.01644	0.02103	0.01538	0.02055

stage. When evaporating the last small fraction of the moisture during the later drying stage, the difficulty of moisture removal for the semidried particles which had different initial moisture contents follows the mother curve.

Aqueous maltodextrin (DE6) droplets

The relative activation energy for the drying of aqueous maltodextrin droplets of 1.5 kg kg^{-1} and 1.0 kg kg^{-1} (dry basis) initial moisture contents is calculated using the same method as for the sucrose droplet. The relative activation energy-moisture content relationship for pure maltodextrin is illustrated in Figure 3. The following correlation was found to be appropriate for fitting experimental relative activation energy data of aqueous maltodextrin (DE6) droplets:

$$\frac{\Delta E_v}{\Delta E_{v,b}} = [1 - C_1(X - X_b)^{C_2}] \exp(-C_3(X - X_b)^{C_4}) \quad (20)$$

where C_1 , C_2 , C_3 , and C_4 are model coefficients. For aqueous maltodextrin droplets of 1.0 kg kg^{-1} and 1.5 kg kg^{-1} initial moisture concentrations, C_1 , C_2 , C_3 , and C_4 are listed in

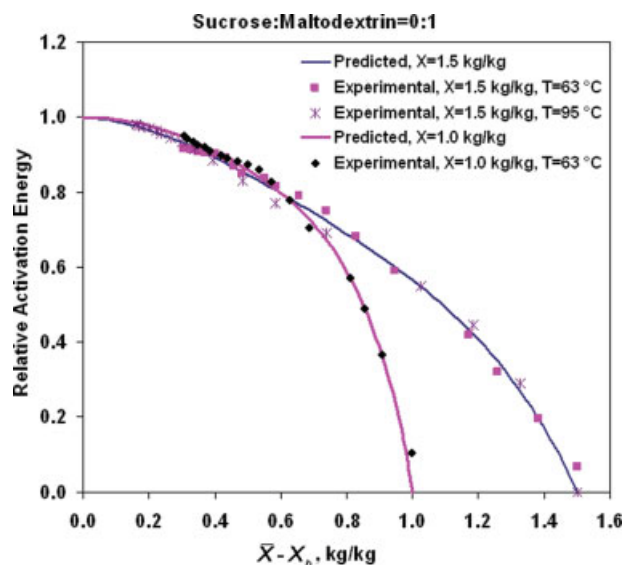


Figure 3. Experimental relative activation energy and fitted curves for the drying of aqueous maltodextrin droplets (S:M = 0:1) using 63 and 95°C air temperature conditions.

[Color figure can be viewed in the online issue, which is available at www.interscience.wiley.com.]

Table 5. Again, the relative activation energy curves for the droplets of $X_0 = 1.5 \text{ kg kg}^{-1}$ and $X_0 = 1.0 \text{ kg kg}^{-1}$ were distinctively different when removing the first fraction of the moisture (see Figure 3). The relative activation energy curve as well as experimental relative activation energy data for the droplet of $X_0 = 1.0 \text{ kg kg}^{-1}$ observed to be merging with the mother curve (i.e. the relative activation curve for the droplet of $X_0 = 1.5 \text{ kg kg}^{-1}$) during the later drying period.

Aqueous sucrose-maltodextrin mixtures

To obtain the relative activation energy-moisture content relationship for the aqueous droplet containing two solutes, sucrose and maltodextrin (DE6), a new “composite” REA is presented in this section. The relative activation energy ($\Delta E_v/\Delta E_{v,b}$) for aqueous droplets of sucrose-maltodextrin mixtures of three different compositions (S:M = 4:1, S:M = 1:1, S:M = 1:4, all weight ratios) was obtained using experimental data. Then $\Delta E_v/\Delta E_{v,b}$ was plotted against corresponding $\bar{X} - X_b$ for the droplets of 1.0 kg kg^{-1} and 1.5 kg kg^{-1} initial moisture contents. Figures 4–6 have shown relative

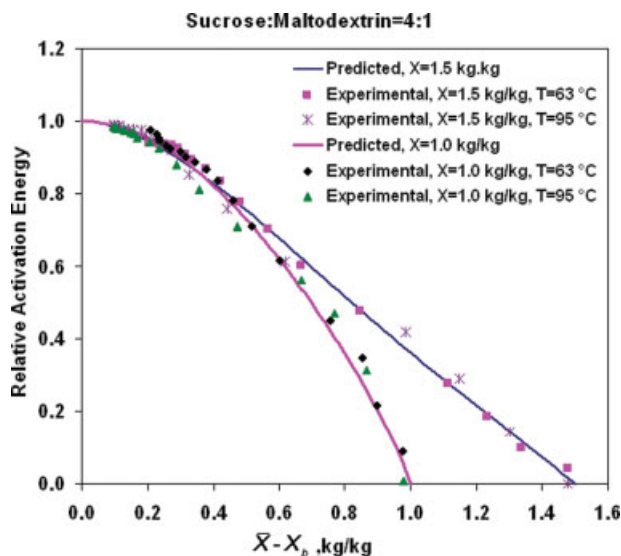


Figure 4. Experimental relative activation energy and fitted curves for the drying of aqueous 80 wt % sucrose – 20 wt % maltodextrin droplets (S:M = 4:1) using 63 and 95°C air temperature conditions.

[Color figure can be viewed in the online issue, which is available at www.interscience.wiley.com.]

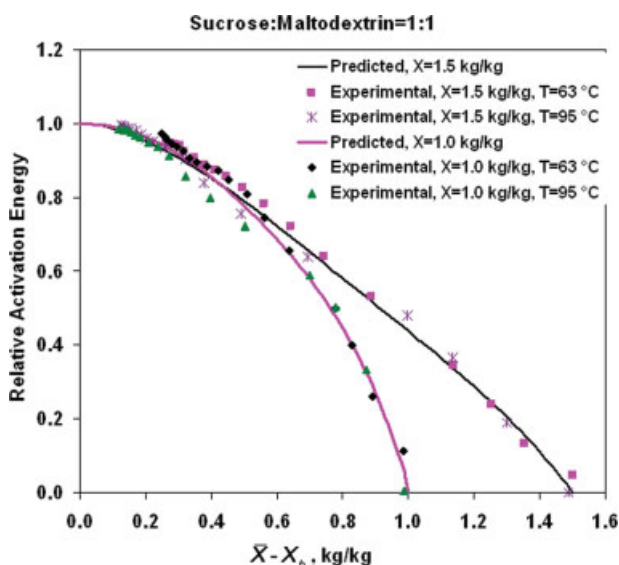


Figure 5. Experimental relative activation energy and fitted curves for the drying of aqueous 50 wt % sucrose – 50 wt % maltodextrin droplets (S:M = 1:1) using 63 and 95°C air temperature conditions.

[Color figure can be viewed in the online issue, which is available at www.interscience.wiley.com.]

activation energy plots for the drying of aqueous droplets of S:M = 4:1, S:M = 1:1 and S:M = 1:4, respectively. The relative activation energy curves for aqueous droplets containing both sucrose and maltodextrin were obtained using the relative activation energy and the mass fraction of each solute:

$$\left(\frac{\Delta E_v}{\Delta E_{v,b}} \right)_{\text{sucrose-maltodextrin}} = \omega_{\text{sucrose}} \left(\frac{\Delta E_v}{\Delta E_{v,b}} \right)_{\text{sucrose}} + \omega_{\text{maltodextrin}} \left(\frac{\Delta E_v}{\Delta E_{v,b}} \right)_{\text{maltodextrin}} \quad (21)$$

where

$$\omega_{\text{sucrose}} + \omega_{\text{maltodextrin}} = 1 \quad (22)$$

When correlating relative activation energy data for the two-solute droplet of $X_0 = 1.5 \text{ kg kg}^{-1}$, equation coefficients C_1 – C_4 corresponding to 1.5 kg kg^{-1} initial moisture contents were used. Figures 4–6 demonstrate that predictions by the composite REA are in good agreement with experimental relative activation energy data for all three sucrose-maltodextrin mixtures and for the droplets of both initial moisture concentrations. The R^2 values were above 0.99 when matching experimental data and relative activation energy curves in Figures 4–6. Again, the relative activation energy curves and experimental relative activation energy data for the droplets of lower initial moisture contents seemed to be merging with the mother curve as drying progressed towards the final stage for each sucrose-maltodextrin mixture. In fact, experimental relative activation energy data on the drying of aqueous skim milk droplets, whole milk droplets and lactose droplets in the

previous studies^{17,18} also exhibited a “merging to a mother curve” behavior as shown in this study. This behavior suggests that the difficulty of moisture removal from the droplets when removing the last small fraction of moisture follows the difficulty of moisture removal projected by the “mother” curve. This behavior of the relative activation energy may be linked with the characteristic behavior of the specific material which will lead to one extreme of the difficulty of moisture removal during drying.

Based on this simple approach, the following composite REA may be suggested for the drying of aqueous droplets containing multiple solutes:

$$\left(\frac{\Delta E_v}{\Delta E_{v,b}} \right)_{\text{mixture}} = \omega_{\text{solute1}} \left(\frac{\Delta E_v}{\Delta E_{v,b}} \right)_{\text{solute1}} + \omega_{\text{solute2}} \left(\frac{\Delta E_v}{\Delta E_{v,b}} \right)_{\text{solute2}} + \omega_{\text{solute3}} \left(\frac{\Delta E_v}{\Delta E_{v,b}} \right)_{\text{solute3}} + \dots \quad (23)$$

To work out the relative activation energy of the droplet containing multiple solutes, the relative activation energy for each solute has to be determined separately as a function of the droplet’s average and initial moisture contents. This composition based approach should however be tested using droplets of more than two solutes to check if the composite REA yields a good fit for each mixture of different solutes.

Discussion

The droplet’s weight loss profiles and average temperature profiles have been predicted using the REA-based drying kinetics model and compared with those obtained from the experimental work of Adhikari et al.^{4,9} The rate of change of

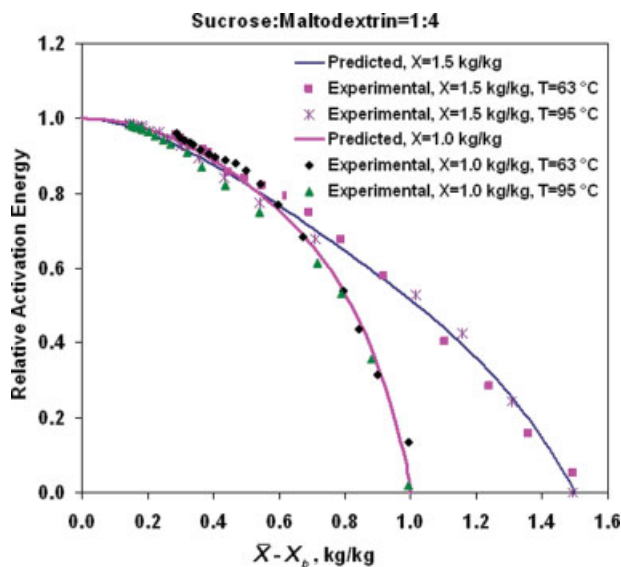


Figure 6. Experimental relative activation energy and fitted curves for the drying of aqueous 20 wt % sucrose – 80 wt % maltodextrin droplets (S:M = 1:4) using 63 and 95°C air temperature conditions.

[Color figure can be viewed in the online issue, which is available at www.interscience.wiley.com.]

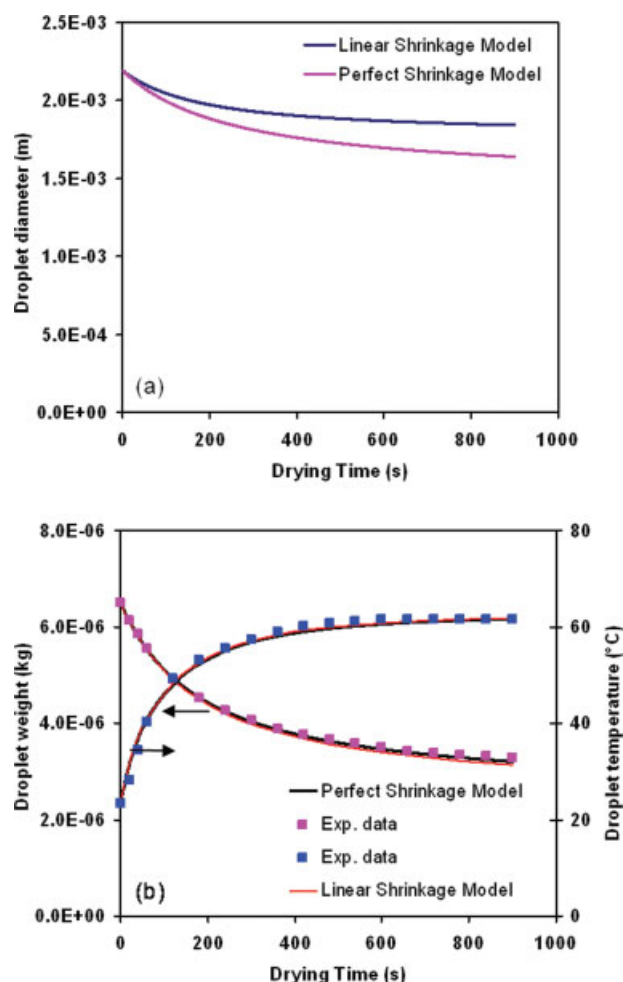


Figure 7. Droplet diameter profiles using the linear shrinkage model and the perfect shrinkage model for the drying of aqueous droplets (S:M = 1:1) of 1.5 kg kg^{-1} initial moisture content and 2.196 mm initial diameter, dried with hot air of 63°C temperature, 2.5 %RH and 1 m s^{-1} velocity.

[Color figure can be viewed in the online issue, which is available at www.interscience.wiley.com.]

the droplet's weight and temperature can be calculated using models presented by Eqs. 5 and 13, respectively once the relative activation energy is estimated using the model described in the previous section. To check the sensitivity of the shrinkage model and its effect on important droplet characteristics, predictions are made here, as an example, for the drying of the aqueous droplet of $X_0 = 1.5 \text{ kg kg}^{-1}$ with total solids of 50 wt % sucrose and 50 wt % maltodextrin (S:M = 1:1). Hot air conditions were 63°C temperature, 2.5 %RH and 1 m s^{-1} velocity (see Table 4). The droplet diameter profiles are predicted using the linear shrinkage model and the perfect shrinkage model. A large variation in the droplet diameter profiles was observed (see Figure 7a) using two shrinkage models. The perfect shrinkage model predicted a lower bound of the droplet diameter, whilst the linear shrinkage model provided a higher bound. To assess the impact of

this deviation of the droplet diameter, the droplet's weight loss and temperature profiles are calculated using both linear and ideal shrinkage models.

Predictions of the droplet's weight and temperature profiles by two shrinkage models are compared with experimental profiles, as shown in Figure 7b. Results in Figure 7b illustrate that a variation in the shrinkage behavior had a small influence on the droplet's temperature and weight loss profiles. The average relative error of the prediction by two shrinkage models is calculated here relative to the droplet characteristics obtained from the experimental work. It was observed that the average relative errors for the droplet's weight loss profiles were 2.0% and 1.0% using the linear and perfect shrinkage models respectively, whilst the average relative errors were 1.83% and 2.14% for the droplet's temperature profiles with the linear and perfect shrinkage models.

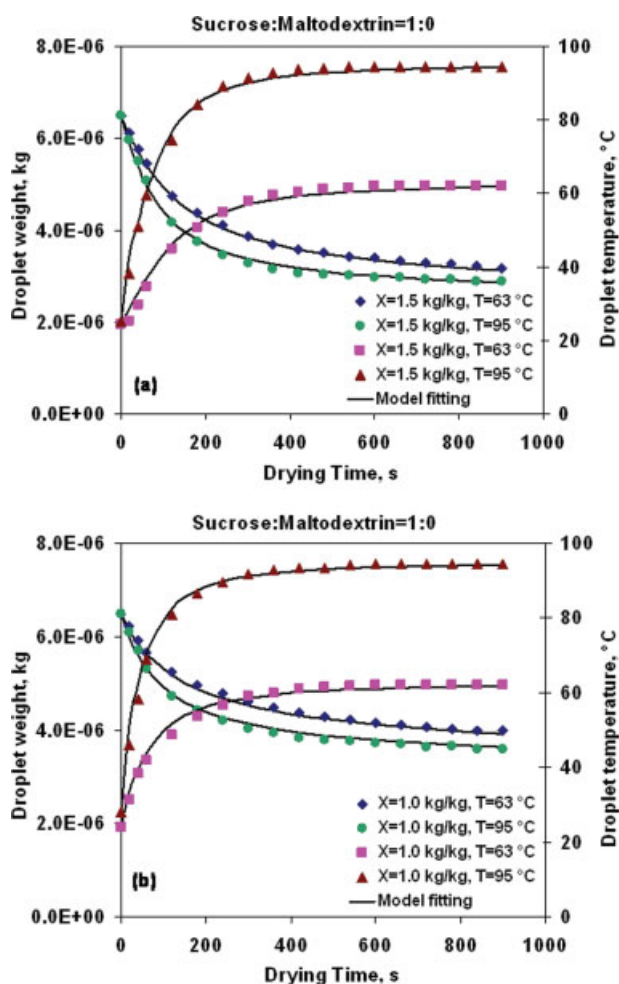


Figure 8. Comparison of experimental data and model predictions using 63°C , 2.5 %RH, and 95°C , 2.0 %RH drying conditions for pure sucrose (S:M = 1:0) droplets of initial characteristics (a) 1.5 kg kg^{-1} moisture content, 2.179-mm diameter (b) 1.0 kg kg^{-1} moisture content, 2.145-mm diameter.

[Color figure can be viewed in the online issue, which is available at www.interscience.wiley.com.]

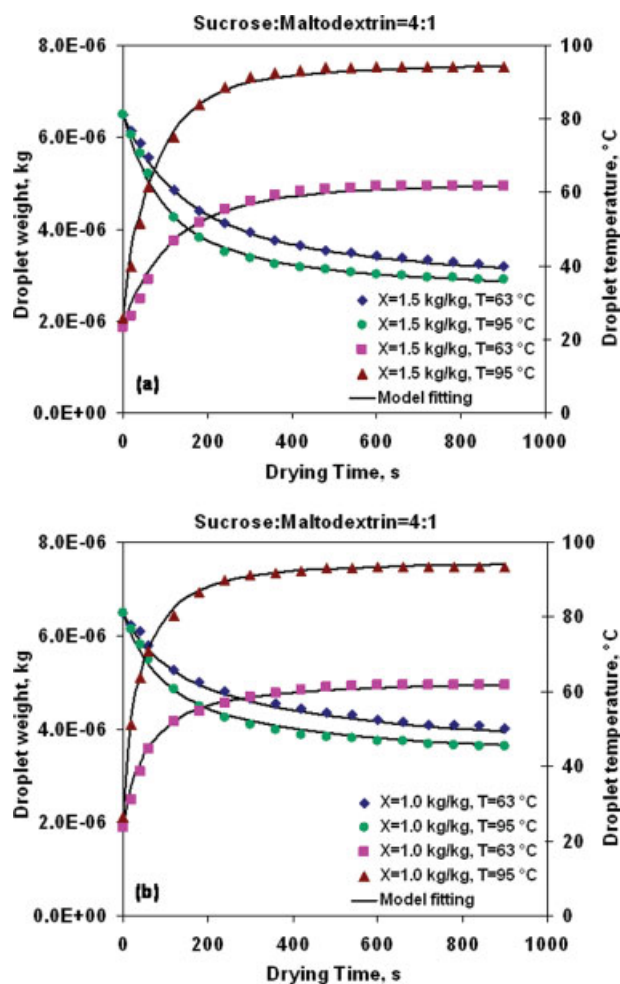


Figure 9. Comparison of experimental data and model predictions using 63°C, 2.5 %RH, and 95°C, 2.0 %RH drying conditions for sucrose-maltodextrin (S:M = 4:1) droplets of initial characteristics (a) 1.5 kg kg⁻¹ moisture content, 2.185-mm diameter (b) 1.0 kg kg⁻¹ moisture content, 2.154-mm diameter.

[Color figure can be viewed in the online issue, which is available at www.interscience.wiley.com.]

Because the accuracy of prediction was slightly better for the perfect shrinkage model compared to the accuracy for the linear shrinkage model, the perfect shrinkage model is used to predict droplet properties for the rest of simulation runs in this study. It is recommended that empirical shrinkage models such as the linear model should be formulated based on accurate measurements of the droplet diameter profile from the droplet drying process, unlike based on the droplet diameter at the starting and end points only as has been done in this study. This aspect however will not diminish the importance of the composite REA.

Figures 8–12 have illustrated experimental and predicted droplet weight and temperature profiles during the convective drying of aqueous droplets containing sucrose and maltodextrin with solute proportions (S:M) of 1:0, 4:1, 1:1, 1:4, and 0:1, respectively. The average relative errors (%) when

matching predicted data and experimental data are calculated with respect to experimental data, and presented in Table 6 for each drying case. Figures 8–12 and Table 6 reveal that for the droplets of $X_0 = 1.5 \text{ kg kg}^{-1}$, the average relative error when matching the droplet's weight loss profiles is in the range of 0.87–1.41%, whilst the average relative error for the temperature prediction was around 0.7–3.0%. For the droplets of $X_0 = 1.0 \text{ kg kg}^{-1}$, the average relative errors for the droplet's weight and temperature predictions were in the range of 0.6–1.5% and 0.3–2.0%, respectively. The accuracy of prediction was slightly higher for the droplets of 1.0 kg kg⁻¹ initial moisture contents compared to that of 1.5 kg kg⁻¹ initial moisture contents. In general, model predictions and experimental data are in good agreement. The accuracy of prediction by the REA-based drying kinetics model, which accounted for the droplet's initial moisture content, is high.

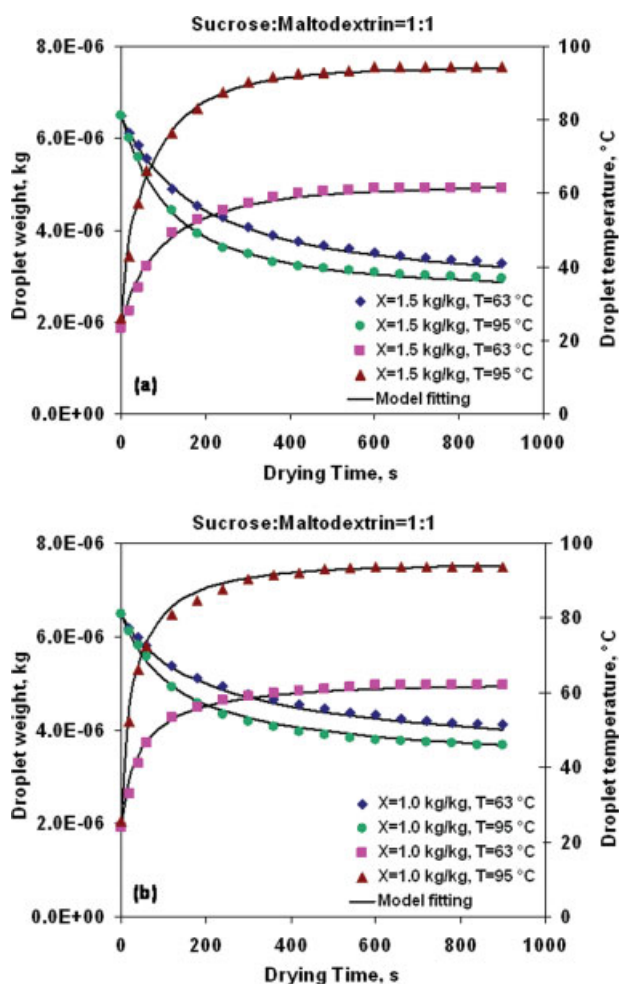


Figure 10. Comparison of experimental data and model predictions using 63°C, 2.5 %RH, and 95°C, 2.0 %RH drying conditions for sucrose-maltodextrin (S:M = 1:1) droplets of initial characteristics (a) 1.5 kg kg⁻¹ moisture content, 2.196-mm diameter (b) 1.0 kg kg⁻¹ moisture content, 2.167-mm diameter.

[Color figure can be viewed in the online issue, which is available at www.interscience.wiley.com.]

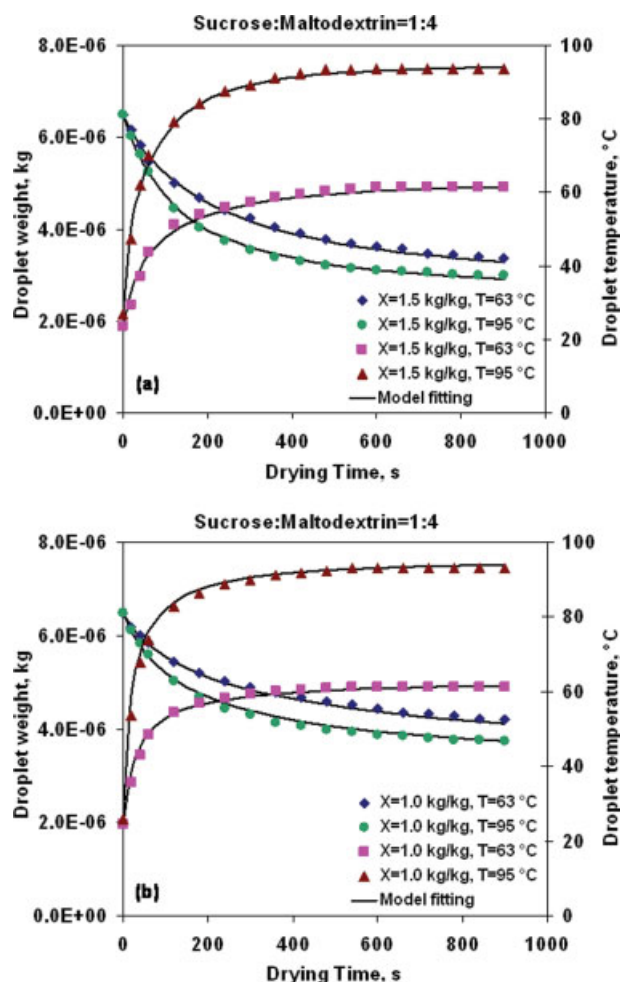


Figure 11. Comparison of experimental data and model predictions using 63°C, 2.5 %RH, and 95°C, 2.0 %RH drying conditions for sucrose-maltodextrin (S:M = 1:4) droplets of initial characteristics (a) 1.5 kg kg⁻¹ moisture content, 2.206-mm diameter (b) 1.0 kg kg⁻¹ moisture content, 2.180-mm diameter.

[Color figure can be viewed in the online issue, which is available at www.interscience.wiley.com.]

Outcomes from this simulation also illustrate that the average relative error by the REA-based drying kinetics model is smaller than the diffusion-based drying kinetics model proposed by Adhikari et al.^{4,9} for the same droplet and drying conditions used in this study.

Possible sources for the inaccuracy of prediction in this work could be an inappropriate shrinkage model, errors in measuring droplet characteristics and air conditions from the experimental work and errors in estimating important thermo-physical properties such as equilibrium moisture content (X_b). The accuracy of prediction also relies on how accurately relative activation energy data are fitted to obtain the characteristic relative activation energy-moisture content relationship for the specific material. Furthermore, the assumption of a spherical droplet during the entire drying period may not be a good one because the experimental work of

Adhikari et al.^{4,9} showed that the sucrose-maltodextrin droplet developed wrinkles and folds on the droplet surface during drying.

Adhikari et al.^{4,9} reported the accuracy when measuring temperature and relative humidity of hot air from the experimental work to be $63 \pm 1^\circ\text{C}$ with 2.5 ± 0.5 %RH and $95 \pm 2^\circ\text{C}$ with 2.0 ± 0.5 %RH. The sensitivity of prediction by the REA with respect to the accuracy of air temperature and air relative humidity is also assessed here. The simulation run is conducted for the drying of sucrose-maltodextrin (S:M = 1:1) droplets ($X_0 = 1.5$ kg kg⁻¹) using hot air of $95 \pm 2^\circ\text{C}$ temperature and 2.0 ± 0.5 %RH. Predictions are made for 93 and 97°C air temperature conditions while keeping the air RH to be 2.0%, and compared with the 95°C temperature condition. It was observed from Figure 13a that 93°C and 97°C air temperature conditions either underpredict

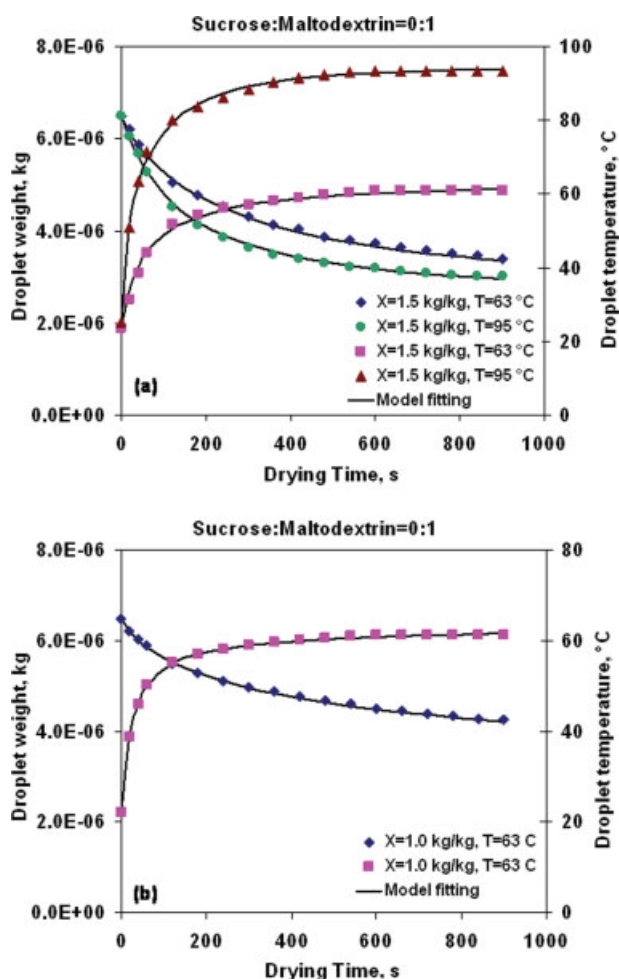


Figure 12. Comparison of experimental data and model predictions using 63°C, 2.5 %RH, and 95°C, 2.0 %RH drying conditions for pure maltodextrin (S:M = 0:1) droplets of initial characteristics (a) 1.5 kg kg⁻¹ moisture content, 2.214-mm diameter (b) 1.0 kg kg⁻¹ moisture content, 2.188-mm diameter.

[Color figure can be viewed in the online issue, which is available at www.interscience.wiley.com.]

Table 6. Average Relative Error When Matching Predicted and Experimental Droplet Temperature and Weight Profiles for the Droplet Drying Cases Presented in Table 4

S:M Weight Ratio	Air Temp. (°C)	Average Relative Error (%) for Droplet Weight		Average Relative Error (%) for Droplet Temperature	
		$X_0 = 1.5 \text{ (kg kg}^{-1}\text{)}$	$X_0 = 1.0 \text{ (kg kg}^{-1}\text{)}$	$X_0 = 1.5 \text{ (kg kg}^{-1}\text{)}$	$X_0 = 1.0 \text{ (kg kg}^{-1}\text{)}$
1:0	63	0.92	1.25	2.97	1.92
	95	1.41	1.49	1.69	1.81
4:1	63	0.87	1.49	2.55	1.55
	95	1.16	1.47	1.66	0.76
1:1	63	0.97	1.37	2.14	1.63
	95	1.20	1.31	1.33	1.18
1:4	63	1.10	1.12	2.16	1.28
	95	1.15	1.34	1.08	1.33
0:1	63	0.94	0.61	1.35	0.29
	95	1.05	—	0.68	—

or overpredict the droplet's temperature and weight profiles. The REA is found to be sensitive to the air temperature accuracy. Predictions are also made for 1.5 and 2.5 %RH con-

ditions while keeping the air temperature to be 95°C. The model is found to be less sensitive to a small inaccuracy in the air RH measurement, as shown by predicted profiles in Figure 13b.

In general, it was observed that the REA-based drying kinetics model is sensitive to the accuracy of the experimental measurement. The average relative error in the prediction was small and may be further reduced when a more accurate shrinkage model, the experimental heat-mass transfer surface area and the precise measurement of the droplet and air characteristics are employed in the simulation. The influence of the extent of the average relative error on the prediction should be checked under “actual” spray drying conditions before employing the drying kinetics model into dryer-wide simulations for industrial operations. The REA-based drying kinetics model has provided a simple and effective framework for correlating drying data of aqueous droplets containing single solutes as well as two solutes. The REA-based drying kinetics model that takes into account for the initial moisture content effect should be used for future dryer-wide simulations for industrial spray drying operations.

For the drying of sugar droplets containing two solutes, the success of the composite REA (i.e. the additive approach based on solute weight fractions) may be related to the “uniform” mixing behavior or the “homogeneity” of sucrose and maltodextrin molecules within the aqueous droplet. It would be interesting to assess the performance of the composite REA (Eq. 23) for the drying of aqueous droplets, e.g. milk droplets, which contain solutes such as carbohydrates (lactose), fat, proteins, and minerals which largely differ in their water binding activity, solubility, and other molecular characteristics (e.g. size and shape). It is expected that the additive approach based on solute weight fractions to account for the individual contribution by each solute may not be as straightforward as illustrated for sugar droplets having two solutes. The composite REA should be tested against a wide range of mixtures of different solutes using relevant drying and feed conditions in order to assess the versatility of the model.

Conclusions

In this study, the REA-based drying kinetics model is formulated for the drying of aqueous sugar solutions containing single solutes as well as two solutes. A simple “composite” REA is found to be suitable for describing the drying behav-

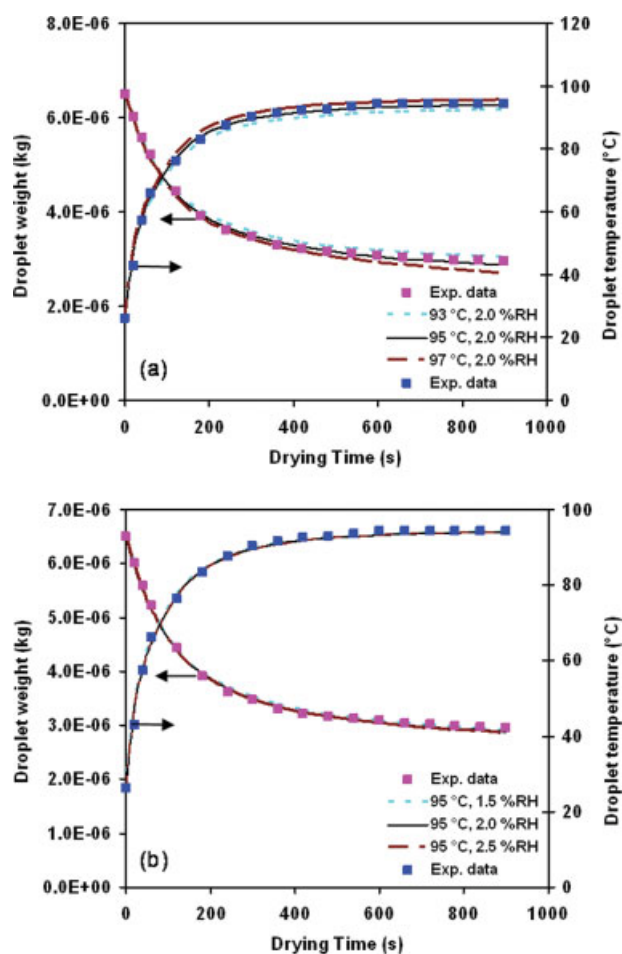


Figure 13. Sensitivity analysis to check the effect of variations in the experimental measurement on particle characteristics for the sucrose-maltodextrin droplet (S:M = 1:1) of $X_0 = 1.5 \text{ kg kg}^{-1}$ dried using hot air of $95 \pm 2^\circ\text{C}$ temperature and $2.0 \pm 0.5\%$ relative humidity.

[Color figure can be viewed in the online issue, which is available at www.interscience.wiley.com.]

ior of two solute mixtures of different solute proportions. This additive approach may be extended to model the drying behavior of aqueous droplets containing multiple solutes having similar molecular characteristics. This first attempt on formulating the composite REA has provided a platform for exploring more extensive applications of the reaction engineering approach. Results demonstrated that the REA is sensitive to the accuracy of experimental measurements and required a carefully controlled data measurement system in order to formulate an accurate drying kinetics model. The drying kinetics model formulated in this study can readily be incorporated into computation tools such as CFD for simulating industrial spray drying operations. It is believed that the composite REA-based drying kinetics model can be employed not only to the drying of food and dairy materials but may also be used for the drying of other porous and nonporous materials where convection and evaporation are significant.

Acknowledgments

Kamlesh C. Patel thanks Chemical Engineering Department of Monash University for offering the scholarship in the last phase of candidature. Authors sincerely appreciate the Australian Research Council Discovery Grant (DP0773688) for supporting part of this work.

Notation

Letters

a_w = water activity
 A = surface area, m^2
 C_i = equation coefficients
 C_p = specific heat capacity, $J\ kg^{-1}\ K^{-1}$
 d = diameter of droplet or particle, m
 D_v = air-vapor diffusion coefficient, $m^2\ s^{-1}$
 ΔE_v = apparent activation energy, $J\ mol^{-1}$
 $\Delta E_{v,b}$ = equilibrium activation energy, $J\ mol^{-1}$
 h = heat transfer coefficient, $W\ m^{-2}\ K^{-1}$
 h_m = mass-transfer coefficient, $m\ s^{-1}$
 ΔH_v = latent heat of vaporization, $J\ kg^{-1}$
 k = thermal conductivity, $W\ m^{-1}\ K^{-1}$
 K_N = Norrish equation coefficient
 m = mass, kg
 Nu = Nusselt number
 Pr = Prandtl number
 R_g = universal gas constant ($8.314\ J\ mol^{-1}\ K^{-1}$)
 RH = relative humidity, %
 Re = Reynolds number
 Sc = Schmidt number
 Sh = Sherwood number
 T = temperature, K
 T_g = glass transition temperature, K
 t = time, s
 \bar{X} = average droplet moisture content, $kg\ kg^{-1}$ (dry basis)
 X_b = equilibrium moisture content, $kg\ kg^{-1}$ (dry basis)
 X_0 = initial moisture content, $kg\ kg^{-1}$ (dry basis)

Greek letters

β = shrinkage model coefficient
 ω = mass fraction
 ρ = density, $kg\ m^{-3}$
 ρ_v = vapor density, $kg\ m^{-3}$
 ψ = molar fraction

Subscripts

b = bulk drying gas
 p = particle, droplet

s = surface conditions
 sat = saturated conditions
 v = vapor
 w = water

Literature Cited

- Bhugra C, Rambhatla S, Bakri A, Duddu SP, Miller DP, Pikal MJ, Lechuga-Ballesteros D. Prediction of the onset of crystallization of amorphous sucrose below the calorimetric glass transition temperature from correlations with mobility. *J Pharm Sci.* 2007;96:1258–1269.
- Roberts CJ, Debenedetti PG. Engineering pharmaceutical stability with amorphous solids. *AIChE J.* 2002;48:1140–1144.
- Aldous BJ, Franks F, Greer AL. Diffusion of water within an amorphous carbohydrate. *J Mater Sci.* 1997;32:301–308.
- Adhikari B, Howes T, Bhandari BR, Troung V. Surface stickiness of drops of carbohydrates and organic acid solutions during convective drying: experiments and modeling. *Drying Technol.* 2003;21:839–873.
- Bhandari BR, Datta N, Howes T. Problems associated with spray drying of sugar-rich foods. *Drying Technol.* 1997;15:671–684.
- Chen XD, Özkan N. Stickiness, functionality and microstructure of food powders. *Drying Technol.* 2007;25:959–969.
- Bhandari BR, Datta N, Cooks R, Howes T, Rigby S. A semiempirical approach to optimize the quantity of drying aids required to spray dry sugar rich foods. *Drying Technol.* 1997b;15:2509–2525.
- Brennan JG, Herrera J, Jowitt R. A study of some of the factors affecting the spray drying of concentrated orange juice on a laboratory scale. *J Food Technol.* 1971;6:295–307.
- Adhikari B, Howes T, Bhandari BR, Troung V. Effect of addition of maltodextrin on drying kinetics and stickiness of sugar and acid-rich foods during convective drying: experiments and modeling. *J Food Eng.* 2004;62:53–68.
- Bhandari BR, Howes T. Implication of glass transition for the drying and stability of foods. *J Food Eng.* 1999;40:71–79.
- Champion D, Le Meste M, Simatos D. Towards an improved understanding of glass transition and relaxations in foods: molecular mobility in the glass transition range. *Trends Food Sci Technol.* 2000;11:41–55.
- Chuy LE, Labuza TP. Caking and stickiness of dairy-based food powders as related to glass transition. *J Food Sci.* 1994;59:43–46.
- Lloyd RJ, Chen XD, Hargreaves JB. Glass transition and caking of spray-dried lactose. *Int J Food Sci Technol.* 1996;31:305–311.
- Roos Y, Karel M. Phase transition of mixture of amorphous polysaccharides and sugars. *Biotechnol Prog.* 1991;7:49–53.
- Schuck P, Blanchard E, Dolivet A, Mejean S, Onillon E, Jeantet R. Water activity and glass transition in dairy ingredients. *Lait.* 2005;85:295–304.
- Chen XD, Xie GZ. Fingerprints of the drying behavior of particulate or thin layer food materials established using a reaction engineering model. *Food Bioprod Process.* 1997;75:213–222.
- Chen XD, Lin SXQ. Air drying of milk droplet under constant and time-dependent conditions. *AIChE J.* 2005;51:1790–1799.
- Lin SXQ, Chen XD. A model for drying of an aqueous lactose droplet using the reaction engineering approach. *Drying Technol.* 2006;24:1329–1334.
- Lin SXQ, Chen XD. The reaction engineering approach to modeling the cream and whey protein concentrate droplet drying. *Chem Eng Process.* 2007;46:437–443.
- Chen XD. The basics of a reaction engineering approach to modeling air-drying of small droplets or thin layer materials. *Drying Technol.* 2008;26:627–639.
- Patel KC, Chen XD. Prediction of spray-dried product quality using two simple drying kinetics models. *J Food Process Eng.* 2005;28:567–594.
- Patel KC, Chen XD. Drying of aqueous lactose solutions in a single stream dryer. *Food Bioprod Process.* 2008;86:185–197.
- Patel KC, Chen XD. Sensitivity analysis of the reaction engineering approach to modeling spray drying of whey proteins concentrate. *Drying Technol.* 2008;26:1334–1343.
- Keey RB. *Drying of Loose and Particulate Materials*. New York: Hemisphere Publishing, 1992.

25. Incropera FP, DeWitt DP. *Fundamentals of Heat and Mass Transfer*, 5th ed. New York: John Wiley, 2002.
26. Lin SXQ, Chen XD. Improving the glass filament method for accurate measurement of drying kinetics of liquid droplets. *Chem Eng Res Des* 2002;80:401–410.
27. Chen XD, Peng X. Modified Biot number in the context of air-drying of small moist porous objects. *Drying Technol.* 2005;23:83–103.
28. Patel KC, Chen XD. Surface-centre temperature differences within milk droplets during convective drying and drying-based Biot number analysis. *AIChE J.* 2008;54:3273–3290.
29. Chen XD. Simultaneous heat and mass transfer. In: Sablani S, Rahman S, Datta, A, Mujumdar AS, editors. *Handbook of Food and Bioprocess Modeling Techniques*. Boca Raton, FL, USA: CRC Press, 2007:179–233.
30. Choi Y, Okos MR. Effects of temperature and composition on the thermal properties of foods. In: Le Maguer M, Jelen P, editors. *Food Engineering and Process Applications*, Vol.1: Transport Phenomena. New York: Elsevier, 1986:93–101.
31. Norrish RS. An equation for the activity coefficients and equilibrium relative humidities of water in confectionary syrups. *Int J Food Sci Technol.* 1966;1:25–39.
32. Toledo RT. Dehydration. In: Heldman DR, editor. *Fundamentals of Food Process Engineering*, 3rd ed. Athens, GA: Springer, 2007: 431–473.
33. Adhikari B. *Drying kinetics and stickiness studies of single drop of sugar and acid-rich solutions*, PhD thesis. The University of Queensland, Australia, 2002.
34. Lin SXQ, Chen XD. Changes in milk droplet diameter during drying under constant drying conditions investigated using the glass-filament method. *Food Bioprod Process.* 2004;82:213–218.
35. Lin SXQ. *Drying of single milk droplets*, PhD thesis. The University of Auckland, New Zealand, 2004.

Manuscript received May 26, 2007, and revision received July 22, 2008.